RESEARCH ARTICLE

Sequence and Structure of a Human Glucose Transporter

Mike Mueckler,* Carla Caruso,† Stephen A. Baldwin
Maria Panico, Ian Blench, Howard R. Morris
W. Jeffrey Allard, Gustav E. Lienhard, Harvey F. Lodish

Abstract. *The amino acid sequence of the glucose transport protein from human HepG2 hepatoma cells was deduced from analysis of a complementary DNA clone. Structural analysis of the purified human erythrocyte glucose transporter by fast atom bombardment mapping and gas phase Edman degradation confirmed the identity of the clone and demonstrated that the HepG2 and erythrocyte transporters are highly homologous and may be identical. The protein lacks a cleavable amino-terminal signal sequence. Analysis of the primary structure suggests the presence of 12 membrane-spanning domains. Several of these may form amphipathic α helices and contain abundant hydroxyl and amide side chains that could participate in glucose binding or line a transmembrane pore through which the sugar moves. The amino terminus, carboxyl terminus, and a highly hydrophilic domain in the center of the protein are all predicted to lie on the cytoplasmic face. Messenger RNA species homologous to HepG2 glucose transporter messenger RNA were detected in K562 leukemic cells, HT29 colon adenocarcinoma cells, and human kidney tissue.*

Most if not all animal cells contain a plasma membrane protein involved in transporting glucose into the cell (*1*). The most extensively studied glucose transport protein (transporter) is the facilitated diffusion carrier of the human erythrocyte (*2*). It is an integral membrane glycoprotein that exhibits an average molecular size of approximately 55,000 daltons on sodium dodecyl sulfate (SDS) polyacrylamide gels and probably contains a single, heterogeneous, *N*-linked oligosaccharide. The purified erythrocyte transporter demonstrates specific D-glucose transport activity when reconstituted into lipid vesicles (*2*).

The rapid increase in glucose uptake in muscle and fat cells triggered by insulin is of considerable interest. In both cell types, insulin appears to induce the rapid translocation of glucose transporters from an intracellular storage pool to the plasma membrane, thus increasing glucose uptake by the cells (*3*). In adipocytes, insulin may also decrease the K_m (Michaelis constant) of the transporter for substrate (*4*). The elucidation of the molecular mechanism of this regulation may be crucial to an understanding of the postreceptor defect (or defects) observed in severe insulin unresponsiveness of type II diabetic patients (*5*).

Glucose transporter complementary DNA. Liver cells transport glucose at a high rate via a system of the facilitated diffusion type (*6*). The HepG2 cell line, which is derived from a human hepatoma, exhibits many of the characteristics of differentiated hepatocytes (*7*). Rabbit antiserum to the purified human erythrocyte glucose transporter (molecular weight, 55,000 daltons) cross-reacts with a protein of identical mobility on immuno blots of HepG2 protein extracts resolved by SDS gel electrophoresis (*8*). This antiserum was used to screen a HepG2 complementary DNA (cDNA) library in the expression vector λgt11 (*9*) for recombinant phage that express glucose transporter antigenic determinants (*10*). Four out of 360,000 plaques screened scored positive. Three of these had cDNA inserts that cross-hybridized to each other on Southern blots, and that hybridized to the same messenger RNA (mRNA) species (2850 nucleotides; see Fig. 1) on Northern blots of HepG2 polyadenylated RNA.

As the largest of these inserts was only 1300 base pairs (bp) in length, the λgt11 library was again screened by plaque hybridization; the largest insert was labeled by nick-translation and used as a hybridization probe. Thirty positive plaques were identified out of 500,000 screened. The largest insert fragments of 450 and 2400 bp were found in clone λGT25. These inserts were labeled with ^{32}P by nick-translation and used to probe Northern blots of HepG2 polyadenylated RNA. Both inserts hybridized to the 2850-nt mRNA (Fig. 1). This result indicates that the two inserts correspond to different regions of the same mRNA; it eliminates the possibility that the two inserts represent unrelated cDNA's spliced together during construction of the cDNA library. The total size of the two cDNA inserts was similar to the length of the hybridizing mRNA, indicating that the cDNA contained nearly a full-length copy of the mRNA.

The sequence of λGT25 cDNA is presented in Fig. 2. The initiation codon (residues 1 to 3) was assigned to the first ATG triplet downstream of the in-frame termination codon (TGA) beginning at position −78. An open reading frame starts from this ATG and continues to position 1476. This codes for a 492-residue polypeptide (54,117 daltons). This value is in reasonable agreement with the estimated size of the deglycosylated erythrocyte transporter, 46,000 daltons (*11*). Membrane proteins frequently exhibit increased mobility relative to soluble protein standards on SDS polyacrylamide gels (*12*).

The amino acid composition of the protein deduced from the cDNA sequence is in good agreement with that reported for the purified erythrocyte glucose transporter, and the predicted COOH-terminal valine is consistent with the results of carboxypeptidase digestion of the erythrocyte protein (*13*). Our sequence agrees with that of the first 18 amino acid residues of the erythrocyte transporter reported recently (*14*), in 14 of the 18 residues. Disagreements occur at residues 6, 7, 11, and 13. It is difficult

M. Mueckler is a member of the staff of the Whitehead Institute for Biomedical Research, Nine Cambridge Center, Cambridge, Massachusetts 02142; C. Caruso and S. A. Baldwin are members of the Department of Biochemistry and Chemistry, and of Chemical Pathology and Human Metabolism, Royal Free Hospital School of Medicine, Rowland Hill Street, London NW3 2PF, United Kingdom; M. Panico, I. Blench, and H. R. Morris are members of the Department of Biochemistry, Imperial College, London SW7 2AZ, United Kingdom; W. J. Allard and G. E. Lienhard are members of the Department of Biochemistry, Dartmouth Medical School, Hanover, New Hampshire 03756; H. F. Lodish is a member of the Whitehead Institute for Biomedical Research, Nine Cambridge Center, Cambridge, Massachusetts 02142, and is a professor in the Department of Biology, Massachusetts Institute of Technology, Cambridge 02139.

to assess the significance of the differences observed because the amino acid yields for the cycles of Edman degradation were not reported, and other investigators have described considerable background problems in attempts to sequence from the NH_2-terminus of the intact protein (*13*). However, the results of fast atom bombardment (FAB) analysis of the erythrocyte transporter (described below) are consistent with our assignment of all four of these disputed residues.

Structural analysis of the purified erythrocyte glucose transporter. The glucose transporter of the erythrocyte and HepG2 cells share antigenic determinants and exhibit very similar mobilities on SDS polyacrylamide gels (*15*). We proceeded to determine the extent of their homology and, in the process, to identify the cDNA clone.

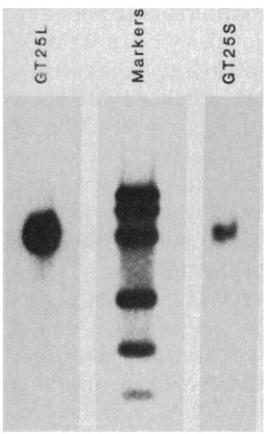

Fig. 1. Size of HepG2 glucose transporter mRNA. Twenty micrograms of HepG2 poly(A) RNA (*10*) were subjected to electrophoresis on a 1.2 percent formaldehyde-agarose gel. As size standards, pBR322 restriction fragments were run in parallel (3611, 3234, 2672, 1691, and 1129 bp). The RNA was blotted and fixed onto nitrocellulose and then hybridized to either a plasmid containing the 450-bp Eco RI cDNA fragment (pGT25S) or the 2400-bp Eco RI cDNA fragment (pGT25L) from λGT25, and labeled with ^{32}P by nick-translation. The hybridization was done at 42°C in 5× SSPE (0.9*M* NaCl, 5 m*M* EDTA, 50 m*M* NaH_2PO_4, *p*H 7.4), 0.2 percent SDS, 0.1 percent each of bovine serum albumin, polyvinylpyrrolidone, and Ficoll; and denatured, sheared salmon sperm DNA (200 μg/ml). The probe was included at 10^7 cpm/ml. After being washed in 0.1× SSPE at 50°C, the blot was exposed to Kodak XAR-5 film at −70°C for 2.5 hours (intensifying screen, DuPont Cronex Lightening Plus).

Table 1. Fast atom bombardment mapping of the erythrocyte glucose transporter. Glucose transporter was purified and delipidated as described (*17*). The delipidated protein (10 mg) in 70 percent (by volume) formic acid was treated with CNBr (10 mg) at ambient temperature for 5 hours in the dark. After dilution with water, the digest was freeze-dried and then resuspended in 50 m*M* ammonium bicarbonate, *p*H 8.4. Trypsin (0.1 mg) was added, and the sample was incubated for 5 hours at 37°C before freeze-drying once more. Edman degradation was carried out on the digest mixture under standard conditions (phenyl isothiocyanate at 45°C followed by cleavage with trifluoroacetic acid for 10 minutes at 45°C). The FAB analysis of peptide digest mixtures was performed with a V.G.ZAB high-field instrument equipped with an M-SCAN fast atom bombardment ion gun as described (*16*). Mass spectra were recorded up to a mass of 3000 amu at full accelerating voltage.

*m/z**	Assignment in deduced amino acid sequence	*m/z**	Assignment in deduced amino acid sequence
446	8 to 11 or 226 to 229†	995	335 to 344
496	Unassigned	1067	Unassigned
524	Unassigned	1118	256 to 264; NH_2-terminal Lys then Val confirmed after two steps of Edman
574	7 to 11; NH_2-terminal Lys confirmed after one step of Edman		
588	Unassigned	1142	459 to 468; NH_2-terminal Thr then Phe confirmed after two steps of Edman
610	Unassigned		
630	345 to 351; lactone		
642	8 to 13; lactone	1146	Unassigned
660	8 to 13	1170	Unassigned
718	Unassigned	1191	Unassigned
736	111 to 117	1268	233 to 244; lactone, NH_2-terminal Gly then Thr confirmed after two steps of Edman
775	213 to 218; NH_2-terminal Phe then Leu or Ile confirmed after two steps of Edman	1286	233 to 244
826	Unassigned	1414	Unassigned
926	78 to 86; NH_2-terminal Leu or Ile then Gly confirmed after two steps of Edman	1537	231 to 244; lactone, NH_2-terminal Leu or Ile confirmed after one step of Edman
929	Unassigned	1555	231 to 244
934	Unassigned	1639	478 to 492; (COOH-terminus), NH_2-terminal Thr then Pro confirmed after two steps of Edman
977	335 to 344; lactone, NH_2-terminal Thr then Leu or Ile confirmed after two steps of Edman		
990	257 to 264; NH_2-terminal Val then Thr confirmed after two steps of Edman	2473	14 to 38
		2480	Unassigned
		2497	469 to 492; (COOH-terminus)

*Essentially the molecular size. †Residues 8 to 11, and so forth.

The structure of the erythrocyte protein was investigated by the technique of FAB mapping (*16*). The FAB mass spectrum of the cyanogen bromide (CNBr)–tryptic digest of the protein yielded a number of strong signals corresponding to quasi-molecular ions $[M + H]^+$. A computer search for the peptide masses within the predicted amino acid sequence revealed that most of the ions had masses expected for CNBr–tryptic fragments of the protein (Table 1). Some peaks do not correspond to expected fragments unless we assume the action of nonspecific proteolytic or acid cleavage. These peaks have not been assigned in Table 1, but may in fact be derived from the protein as evidenced by computer matches of the mass of the peptides to regions of the predicted sequence. Signal assignments were confirmed by comparing the spectra of the digest after up to two cycles of Edman degradation. The changes in mass observed allowed the identification of the NH_2-terminal and subsequent amino acid in many cases, and enabled the position of the fragments within the predicted sequence to be assigned unambiguously. Approximately 26 percent of the predicted sequence was mapped by this analysis. In particular, the predicted sequence of residues 7 to 38 was confirmed completely, and thus the protein has no cleaved signal sequence at the NH_2-terminus. The isolation of peptides 469 to 492 and 478 to 492 shows that there is no proteolytic processing at the carboxyl terminus either.

In a 15,000- to 20,000-dalton protein we might map 90 percent of the sequence, but in a larger molecule and, in particular, one heavily contaminated with lipid and carbohydrate, a lower proportion will be observed due to suppression phenomena, as described by Morris *et al.* (*16*). The presence of covalently attached oligosaccharides may also restrict proteolytic cleavage, as may solubility problems resulting from the hydrophobic nature of the protein. In addition, the predicted sequence shows that several regions of the protein would, upon digestion, yield fragments too large to have been detected in our study.

An analysis was also conducted on two peptides purified by reversed-phase high-performance liquid chromatography after tryptic digestion of the native transporter reconstituted into lipid vesicles (*17*). These gave signals at *m/z* 1142 and 1444 when analyzed by FAB mass spectrometry, corresponding to amino acid residues 459 to 468, and 233 to 245, respectively. These peptides were sequenced completely by gas phase Edman

degradation, and both sequences agreed precisely with their assignment in the cDNA sequence (see Fig. 2, underlined sequences). We conclude that the erythrocyte and HepG2 glucose transporters are extremely similar, if not identical.

HepG2 glucose transporter cDNA was used to probe a Northern blot of polyadenylated RNA isolated from four other human cell lines or tissues (Fig. 3). RNA species homologous to HepG2 glucose transporter mRNA were detected in the leukemic cell line K562 (*18*), the colon adenocarcinoma cell line HT29 (*19*), and cortical and medullary kidney tissue. Thus, it is likely that a facilitated diffusion glucose transporter similar to that found in erythrocytes is also expressed in these cells or tissues.

Structure of the glucose transporter. Our results indicate that the glucose transporter of HepG2 cells is highly homologous, if not identical, to the erythrocyte transporter. In addition to the structural evidence described above, β-galactosidase fusion proteins produced by some of the isolated λgt11 cDNA clones reacted with three distinct monoclonal antibodies directed against the erythrocyte glucose transporter (*15*), as well as the polyclonal antiserum. Thus it is extremely unlikely that the 55,000-dalton polypeptide isolated from erythrocytes, which exhibits glucose transport activity in vitro, arises from the proteolysis of a much larger erythrocyte membrane protein, as has been suggested (*20*). No homology was observed between the amino acid sequence of the glucose transporter and the recently elucidated sequence of murine erythrocyte band III protein (*21*), as has been postulated by some investigators (*22*).

Both the 3′ and 5′ untranslated regions of the glucose transporter mRNA are unusually long (at least 1197 and 179 residues, respectively). The 5′ untranslated region is also unusually GC rich (73 percent), with the potential for extensive secondary structure formation. Figure 4 illustrates the most stable predicted hairpin-loop structure, and a hypothetical interaction between a sequence of five bases in the loop structure and the 3′ end of 18*S* ribosomal RNA (rRNA). The combined structure has a predicted stability of −37.0 kcal/mol (*23*). An interaction of this type has been proposed for several other eukaryotic mRNA's (*24*), although the stability of the proposed structures is seldom as great as that shown in Fig. 4. It has been suggested that an interaction of this type may function in the initiation of translation, or the regulation of this process, for some eukaryotic mRNA's (*24*).

A hydropathy plot of the deduced amino acid sequence obtained by the method of Kyte and Doolittle (*25*) is presented

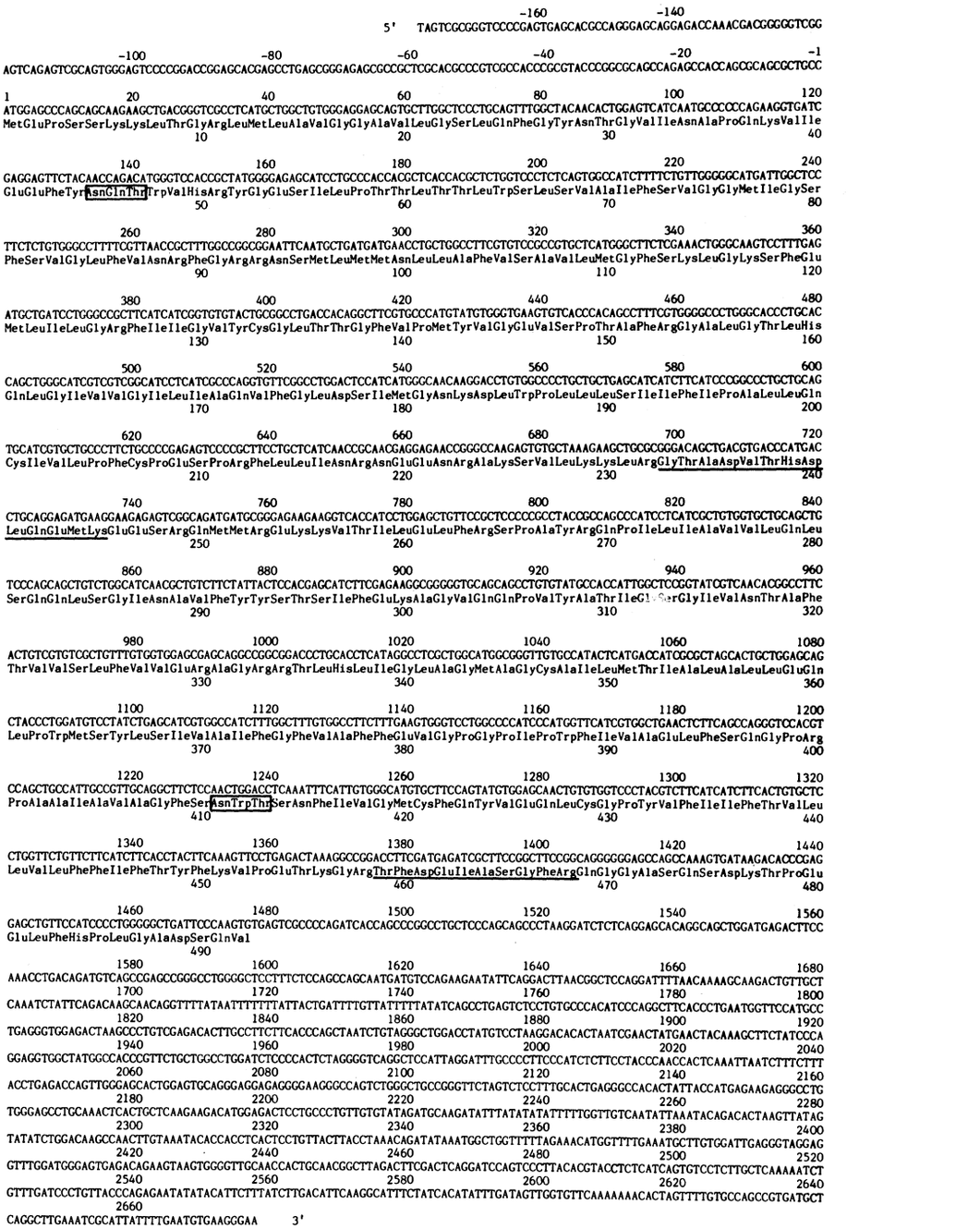

Fig. 2. Nucleotide sequence of λGT25 cDNA and deduced sequence of the HepG2 glucose transporter. Numbering of nucleotides is above the sequence and the numbering of amino acid residues is below. The tryptic peptides sequenced by Edman degradation are underlined. The two potential sites of *N*-linked glycosylation (Asn-X-Ser or Thr, where X is any amino acid) are boxed. The Eco RI linker sequences at the 5′ and 3′ termini are not included in the sequence. The two Eco RI cDNA fragments (from λGT25) of 450 bp and 2400 bp were subcloned into plasmids, and designated pGT25S and pGT25L, respectively. After Eco RI digestion of the plasmids and subsequent agarose gel electrophoresis, the cDNA inserts were isolated and self-ligated with T4 DNA ligase. The resulting concatomers were sonicated, and the fragments of 300 to 1000 bp were isolated after agarose gel electrophoresis. The fragments were incubated with T4 DNA polymerase (to create blunt ends), and then subcloned into the Sma I sites of M13 mp18 and mp19 (*31*). The cDNA inserts were sequenced according to a modified version (*32*) of the method of Sanger *et al.* (*33*). Sequence data were analyzed by means of the computer-assisted method of Staden (*34*). The DNA was sequenced completely in both strands with an average of 5.7 gel readings per residue. A 687-bp Hinc II fragment (residues 262 to 948) was subcloned from λGT25 and sequenced to confirm the nucleotide sequence in the region of the Eco RI site between positions 279 and 280.

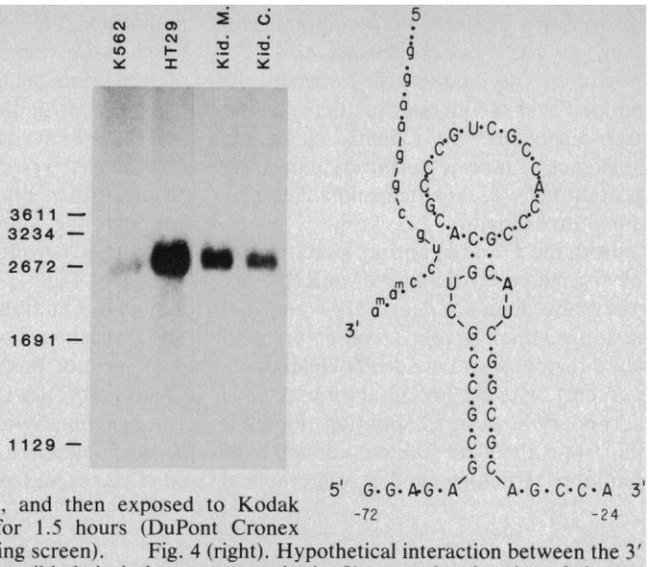

Fig. 3 (left). Detection of glucose transporter mRNA in human cell lines and tissues. The following quantities of human polyadenylated RNA's were analyzed by Northern gel blot analysis (as described in the legend to Fig. 2): for K562 leukemic cells (*18*), 10 μg; for HT29 adenocarcinoma cells (*19*), 10 μg; for kidney medulla, 20 μg; kidney cortex, 20 μg. The blot was hybridized to pGT25S and pGT25L cDNA's labeled with ^{32}P by nick-translation, washed, and then exposed to Kodak XAR-5 film at −70°C for 1.5 hours (DuPont Cronex Lightening Plus intensifying screen). Fig. 4 (right). Hypothetical interaction between the 3′ end of 18*S* rRNA and a possible hairpin-loop structure in the 5′ untranslated region of glucose transporter mRNA. The lowercase letters represent the sequence of the 3′ end of eukaryotic 18*S* rRNA (*35*). The conformation of the hairpin-loop structure is arranged for maximum stability as estimated by the method of Tinocco *et al.* (*23*).

in Fig. 5 (left panel), along with a speculative model for the membrane orientation of the glucose transporter (right panel). The model is based on a number of computer and graphical analyses of the predicted protein sequence and on the results of chemical and proteolytic digestion experiments performed on the native, membrane-bound protein.

Analysis of the sequence according to the algorithm of Eisenberg *et al.* (*26*) predicts the presence of 12 membrane-spanning segments. This algorithm assigns all nonoverlapping segments of 21 amino acid residues having an average hydropathy value of >0.42 as membrane-spanning domains. The assigned segments are numbered 1 through 12 in the hydropathy plot and in the model. Exact assignments for the termini of the membrane-spanning domains is given in the model only to facilitate the following discussion. The average hydropathy of the assigned segments, according to the hydropathy scale in (*26*), ranged from 0.52 (segment 7) to 0.89 (segment 12). It is assumed in this model that membrane-spanning domains comprise α-helical segments of about 21 amino acid residues (*26*). The presence of β turns in the hydrophilic loops separating the proposed membrane-spanning domains is predicted by analysis of the sequence according to the method of Chou and Fasman (*27*). Graphical representation of the membrane-spanning segments indicates that segments 3, 5, 7, 8, and 11 may form amphipathic α helices. These contain several serine, threonine, glutamine, and asparagine residues that would largely be localized to the same face of the α helix. The hydroxyl and amide side chains in a glucose transporter membrane domain may line the transmembrane channel and could play key roles in specific binding of hexoses. The glucose transporter appears to lack a strongly amphipathic transmembrane segment containing several charged residues, as has been predicted for some ion channel proteins (*21, 28*).

The glucose transporter in intact erythrocytes and sealed erythrocyte ghosts is resistant to tryptic digestion. It is susceptible to cleavage only at the cytoplasmic surface of the erythrocyte membrane, yielding two large fragments—approximately 23,000 and 18,000 daltons (*11, 29, 30*). The isolation of the tryptic fragment corresponding to residues 233 to 245 after digestion of the membrane-bound transporter (see above) indicates that the extremely hydrophilic domain between residues 207 and 272 is in the cytoplasm. Tryptic cleavage of the reconstituted transporter after residue 458 would reduce the apparent size of the transporter by about 3600 daltons. No change was observed in the apparent size of the protein after

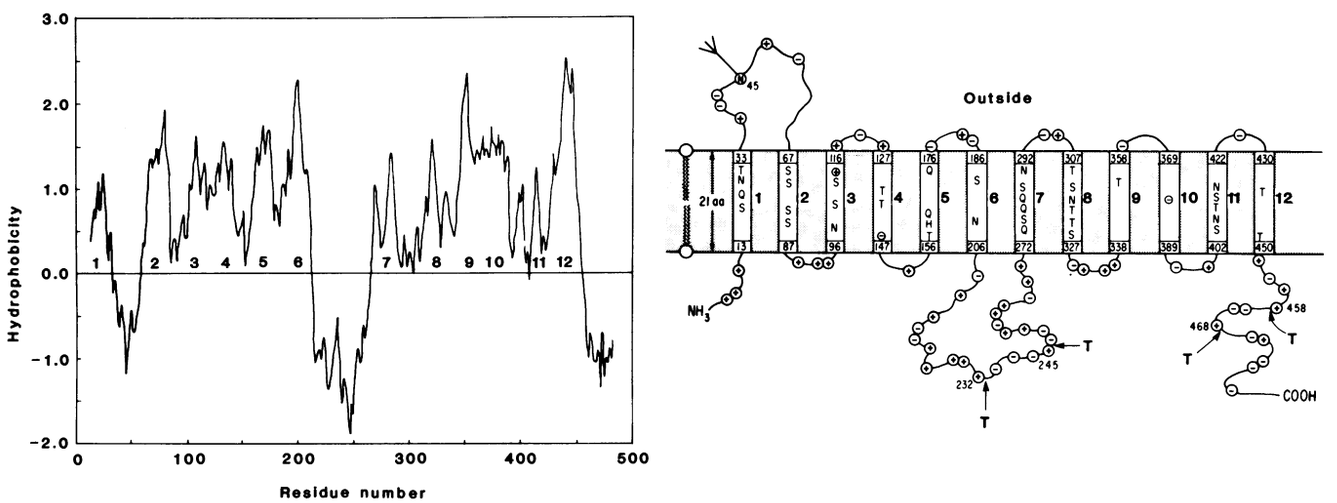

Fig. 5. (Left) Hydropathy plot of the glucose transporter amino acid sequence. Hydropathy values (*25*) for a window of 21 amino acid residues were averaged, assigned to the middle residue of the span, and plotted with respect to position along the amino acid sequence. The numbers refer to putative membrane-spanning domains predicted by the algorithm of Eisenberg *et al.* (*26*). (Right) Proposed model for the orientation of the glucose transporter in the membrane. The 12 putative membrane–spanning domains are numbered and shown as rectangles. The relative positions of acidic (Glu, Asp) and basic (Lys, Arg) amino acid residues are indicated by circled (+) and (−) signs, respectively. Uncharged polar residues within the membrane-spanning domains are indicated by their single-letter abbreviations: S, serine; T, threonine; H, histidine; N, asparagine; Q, glutamine. The predicted position of the *N*-linked oligosaccharide at Asn 45 is shown. The arrows point to the positions of known tryptic cleavage sites in the native, membrane-bound, erythrocyte glucose transporter, as described in the text.

trypsin digestion of intact erythrocytes or sealed ghosts (*11, 30*). This result suggests that the COOH-terminal hydrophilic domain corresponding to residues 451 through 492 is on the cytoplasmic face, but this point must be established directly.

The erythrocyte transporter contains at least one *N*-linked oligosaccharide, which has been localized to either the COOH-terminal or NH_2-terminal third of the molecule (but not at both ends) (*29*). The sequence contains two potential *N*-glycosylation sites, Asn^{45} and Asn^{411}. Thus, only one can be glycosylated. Asn^{411} is predicted to be within a membrane-spanning domain, suggesting that Asn^{45} is glycosylated (Fig. 5). In addition, results of experiments in which the native transporter was cleaved at cysteine residues indicate that a 31,000-dalton fragment corresponding to residues 133 to 420 (or 133 to 428), does not contain carbohydrate (*29*). As this large fragment encompasses the potential glycosylation site at position 411, the actual glycosylation site is assigned to Asn^{45}.

This is substantiated by recent studies in which mRNA's were synthesized in vitro from a full-length cDNA, or a cDNA encoding only the NH_2-terminal 340 amino acids. When translated in a reticulocyte cell-free system in the presence of pancreatic microsomes, both the full-sized and the truncated proteins were inserted into the endoplasmic reticulum membrane, and both were glycosylated at the same site.

The small NH_2-terminal hydrophilic domain (residues 1 to 12) is assigned to the cytoplasmic face since the external loop containing the oligosaccharide (residues 34 to 66) immediately follows the first membrane-spanning domain.

The model presented here disagrees with one proposed recently that was based solely on proteolytic digestion experiments with sealed and unsealed erythrocyte ghosts (*30*). In that model, the COOH-terminus of the transporter is exposed in the extracellular space, and the oligosaccharide is attached near the COOH-terminus. The reasons for this disparity are not evident.

Tissue distribution. The results of the Northern blot experiment shown in Fig. 3 suggest that the facilitated diffusion glucose transporter present in kidney may be the same protein found in both the liver and erythrocytes. The transporter performs a different physiological role in each of these tissues. In erythrocytes, the transporter is responsible for taking up blood glucose for red cell anaerobic glycolysis (*1*). The kidney facilitated diffusion transporter is localized at the basolateral surface of the proximal tubule and is believed to be involved in the transepithelial transport of glucose from the urine to the blood (*36*). The liver protein transports glucose out of the cell during periods of starvation in response to increased intracellular glucose levels resulting from gluconeogenesis and glycogenolysis, and transports glucose into the cell for glycogen storage when blood glucose is high (*6*). Whether the three proteins are, in fact, identical remains to be determined.

The availability of our cDNA clone should make it possible to directly address many important biological questions concerning glucose transport: Is the same or a related transporter found in insulin responsive tissues, that is, fat and muscle? Is the transporter that is expressed constitutively on the surface of insulin responsive cells the same as that recruited from an intracellular storage pool in response to insulin? What region or regions of the protein are necessary for translocation to occur? What regions of the protein are required for substrate binding and transport function? Since the protein lacks a cleaved NH_2-terminal signal sequence, what region (or regions) is involved in initiating proper folding in the membrane?

References and Notes

1. J. Elbrink and I. Bihler, *Science* **188**, 1177 (1975).
2. For reviews, see G. E. Lienhard, J. M. Baldwin, S. A. Baldwin, F. R. Gorga, in *Structure and Function of Membrane Proteins*, E. Quagliariello and F. Palmieri, Eds. (Elsevier, Amsterdam, 1983), pp. 325–333; M. N. Jones and J. K. Nickson, *Biochem. Biophys. Acta* **650**, 1 (1981); T. J. Wheeler and P. C. Hinkle, in *Membranes and Transport*, A. N. Martonosi, Ed. (Plenum, New York, 1982), vol. 2, pp. 161–167.
3. K. Suzuki and T. Kono, *Proc. Natl. Acad. Sci. U.S.A.* **77**, 2542 (1980); S. W. Cushman and L. J. Wardzala, *J. Biol. Chem.* **255**, 4758 (1980); T. Watanabe, M. M. Smith, F. W. Robinson, T. Kono, *ibid.* **259**, 13117 (1984).
4. R. R. Whitesell and N. A. Abumrad, *J. Biol. Chem.* **260**, 2894 (1985).
5. D. W. Foster, in *The Metabolic Basis of Inherited Disease*, J. B. Stanbury *et al.*, Eds. (McGraw-Hill, New York, 1983), pp. 99–117.
6. D. R. F. Elliot and J. D. Craik, *Biochem. Soc. Trans.* **10**, 12 (1981).
7. B. B. Knowles, C. C. Howe, D. P. Aden, *Science* **209**, 497 (1980).
8. G. E. Lienhard, unpublished data; the antiserum used has been described by G. E. Lienhard, H. H. Kim, K. J. Ransome, J. C. Gorga [*Biochem. Biophys. Res. Commun.* **105**, 1150 (1982)]; we thank S. A. Olson and Dr. M. J. Weber for the preparation of the glucose transporter antiserum from antigen supplied by G. E. Lienhard.
9. R. A. Young and R. W. Davis, *Proc. Natl. Acad. Sci. U.S.A.* **80**, 1194 (1983).
10. The HepG2 cDNA library was constructed as follows: Poly(A) RNA was isolated from HepG2 cells by guanidinium thiocyanate-CsCl purification [J. M. Chirgwin, A. W. Przybyla, R. J. MacDonald, W. J. Rutter, *Biochemistry* **18**, 5294 (1979)] followed by oligo(dT) cellulose (deoxythymidylate) chromatography. First strand cDNA synthesis was performed as described [M. M. Mueckler and H. C. Pitot, *J. Cell Biol.* **90**, 95 (1981)]. The second strand was synthesized with the use of DNA polymerase I and ribonuclease H [H. Okayama and P. Berg, *Mol. Cell. Biol.* **2**, 161 (1982)]. The double-stranded cDNA was treated with Eco RI methylase and then ligated to phosphorylated Eco RI linkers. After digestion with Eco RI and Sephadex G-100 chromatography, the cDNA was subjected to electrophoresis on a 1.5 percent agarose gel, and the fraction greater than 600 bp in length was recovered by electroelution. The sample was ligated to Eco RI–digested, phosphatase-treated, λgt11 DNA. The recombinant phage were packaged in vitro and amplified once in *Escherichia coli* Y1088 [R. A. Young and R. W. Davis, *Science* **222**, 778 (1983)]. Screening was conducted with the use of rabbit antiserum to glucose transporter and ^{125}I-labeled protein A as described (*9*).
11. M. R. Deziel and A. Rothstein, *Biochim. Biophys. Acta* **776**, 10 (1984); G. E. Lienhard, J. H. Crabb, K. J. Ransome, *ibid.* **769**, 404 (1984); A. Klip, M. Deziel, D. Walker, *Biochem. Biophys. Res. Commun.* **122**, 218 (1984).
12. S. G. Bonitz, G. Crouzzi, B. E. Thanlenfeld, A. Tzagoloff, G. Macino, *J. Biol. Chem.* **255**, 11927 (1980); L. J. Rizzolo, M. le Maire, J. A. Reynolds, C. Tanford, *Biochemistry* **15**, 3433 (1976).
13. S. A. Baldwin, J. M. Baldwin, G. E. Lienhard, *Biochemistry* **21**, 3836 (1982).
14. P. Lundahl and E. Griejer, *J. Chromatogr.* **297**, 129 (1984).
15. W. J. Allard and G. E. Lienhard, *J. Biol. Chem.* **260**, 3668 (1985).
16. H. R. Morris *et al.*, *Biochem. Biophys. Res. Commun.* **101**, 623 (1981); H. R. Morris, M. Panico, G. W. Taylor, *ibid.* **117**, 299 (1983).
17. Glucose transporter was prepared from outdated human blood as described (*29*). The transporter protein (4 mg) at a concentration of 0.2 mg/ml was digested first at 25°C for 2 hours with diphenylcarbamyl chloride–treated trypsin (40 μg); then 40 μg was added and the digestion was continued for another four hours. The digest was dialyzed against 0.1*M* acetic acid and freeze-dried. Delipidation was performed as described [C. R. Kensil, M. A. Hediger, J. Ozols, P. Stritmatter, *J. Biol. Chem.* **258**, 14656, (1983)]. The delipidated tryptic peptide mixture was fractionated by reversed-phase HPLC on a C-18 column (300-Å pore size); an Altex HPLC system with model 420 solvent programmer was used.
18. C. B. Lozzio and B. B. Lozzio, *Blood* **45**, 321 (1975).
19. K. E. Mostov and G. Blobel, *J. Biol. Chem.* **257**, 11816 (1982).
20. R. E. Mullins and R. G. Langdon, *Biochemistry* **19**, 1205 (1980).
21. R. R. Kopito and H. F. Lodish, *Nature (London)* **316**, 234 (1985).
22. A. Carruthers and D. L. Melchior, *Biochemistry* **23**, 2712 (1984); M. M. B. Kay, *Proc. Natl. Acad. Sci. U.S.A.* **82**, 1731 (1985).
23. I. Tinocco *et al.*, *Nature (London) New Biol.* **246**, 40 (1973).
24. M. B. Gorin, S. B. Yancey, J. Cline, J.-P. Revel, J. Horowitz, *Cell* **39**, 49 (1984); P. Lomedico *et al.*, *ibid.* **18**, 545 (1979).
25. J. Kyte and R. F. Doolittle, *J. Mol. Biol.* **157**, 105 (1982).
26. D. Eisenberg, E. Schwarz, M. Kamaromy, R. Wall, *ibid.* **179**, 125 (1984).
27. P. Y. Chou and G. D. Fasman, *Annu. Rev. Biochem.* **47**, 251 (1978).
28. M. Noda *et al.*, *Nature (London)* **312**, 121 (1984); J. Finer-Moore and R. M. Stroud, *Proc. Natl. Acad. Sci. U.S.A.* **81**, 155 (1984).
29. M. T. Cairns, D. A. Elliot, P. R. Scudder, S. A. Baldwin, *Biochem. J.* **221**, 179 (1984).
30. M. F. Shanahan and J. D'Artel-Ellis, *J. Biol. Chem.* **259**, 13878 (1984).
31. J. Norrander, T. Kempe, J. Messing, *Gene* **26**, 101 (1983).
32. M. D. Biggin, T. J. Gibson, G. F. Hong, *Proc. Natl. Acad. Sci. U.S.A.* **74**, 5463 (1983).
33. F. Sanger, S. Nicklen, A. R. Coulson, *ibid.*, p. 74.
34. R. Staden, *Nucleic Acids Res.* **10**, 4731 (1982).
35. O. Hagenbuchle, M. Santer, J. A. Steitz, R. J. Mans, *Cell* **13**, 551 (1978).
36. M. Silverman, in *Membranes and Transport*, A. N. Martonosi, Ed. (Plenum Press, New York, 1982), vol. 2, pp. 207–216.

37. Supported by NIH grant HL32262 (H.F.L.), a postdoctoral fellowship from the Damon Runyon–Walter Winchell Cancer Fund (DRG-711) (M.M.); NIH grant GM22996 (G.E.L.); Medical Research Council financial aid for the I.C. protein chemistry facility, and a grant (S.A.B.); and the Wellcome Trust for a research fellowship (C.C.). We thank Piero Pucci for assistance in the early mass spectrometric analysis.

* To whom correspondence should be addressed.
† Present address: Instituto Internazionale di Genetica e Biofisica, Consiglio Nazionale delle Ricerche, Via Guglielmo Marconi 10-80125 Napoli, Italy.

17 May 1985; accepted 2 August 1985